blood®

Regular Article

TRANSPLANTATION

Neutrophils provide cellular communication between ileum and mesenteric lymph nodes at graft-versus-host disease onset

Jan Hülsdünker,[1-3] Katja J. Ottmüller,[4,5] Hannes P. Neeff,[6] Motoko Koyama,[7,8] Zhan Gao,[9] Oliver S. Thomas,[1-3] Marie Follo,[1] Ali Al-Ahmad,[10] Gabriele Prinz,[1] Sandra Duquesne,[1] Heide Dierbach,[1] Susanne Kirschnek,[11] Tim Lämmermann,[12] Martin J. Blaser,[9] Brian T. Fife,[13] Bruce R. Blazar,[14] Andreas Beilhack,[4,15,16] Geoffrey R. Hill,[7,8] Georg Häcker,[11,*] and Robert Zeiser[1,*]

[1]Department of Hematology, Oncology and Stem Cell Transplantation, Freiburg University Medical Center, Albert Ludwigs University Freiburg, Freiburg, Germany; [2]Spemann Graduate School of Biology and Medicine and [3]Faculty of Biology, University Freiburg, Freiburg, Germany; [4]Interdisciplinary Center for Clinical Research Würzburg, Würzburg, Germany; [5]Department of Hematology and Oncology, University of Würzburg Graduate School of Life Sciences, Würzburg, Germany; [6]Clinic of General and Visceral Surgery, Department of Surgery, University Medical Center Freiburg, Freiburg, Germany; [7]Department of Immunology, QIMR Berghofer Medical Research Institute, Brisbane, QLD, Australia; [8]School of Medicine, University of Queensland, Herston, QLD, Australia; [9]Department of Medicine, New York University Langone Medical Center, New York, NY; [10]Department of Operative Dentistry and Periodontology, Center for Dental Medicine, Albert-Ludwigs University, Freiburg, Germany; [11]Institute of Medical Microbiology and Hygiene, University Medical Center Freiburg, Freiburg, Germany; [12]Group Immune Cell Dynamics, Max Planck Institute of Immunobiology and Epigenetics, Freiburg, Germany; [13]Department of Medicine and Center for Immunology and [14]Division of Blood and Marrow Transplantation, Masonic Cancer Center and Department of Pediatrics, University of Minnesota, Minneapolis, MN; [15]Else-Kröner-Forschungskolleg for Interdisciplinary Translational Immunology, Würzburg, Würzburg, Germany; and [16]Department of Medicine II, Würzburg University Clinics, Würzburg, Germany

KEY POINTS

- **Neutrophils migrate to the ileum after conditioning and contribute to GVHD.**
- **JAK1/JAK2 inhibition reduces neutrophil influx and MHC-II expression in the mesenteric lymph node.**

Conditioning-induced damage of the intestinal tract plays a critical role during the onset of acute graft-versus-host disease (GVHD). Therapeutic interference with these early events of GVHD is difficult, and currently used immunosuppressive drugs mainly target donor T cells. However, not donor T cells but neutrophils reach the sites of tissue injury first, and therefore could be a potential target for GVHD prevention. A detailed analysis of neutrophil fate during acute GVHD and the effect on T cells is difficult because of the short lifespan of this cell type. By using a novel photoconverter reporter system, we show that neutrophils that had been photoconverted in the ileum postconditioning later migrated to mesenteric lymph nodes (mLN). This neutrophil migration was dependent on the intestinal microflora. In the mLN, neutrophils colocalized with T cells and presented antigen on major histocompatibility complex (MHC)-II, thereby affecting T cell expansion. Pharmacological JAK1/JAK2 inhibition reduced neutrophil influx into the mLN and MHC-II expression, thereby interfering with an early event in acute GVHD pathogenesis. In agreement with this finding, neutrophil depletion reduced acute GVHD. We conclude that neutrophils are attracted to the ileum, where the intestinal barrier is disrupted, and then migrate to the mLN, where they participate in alloantigen presentation. JAK1/JAK2-inhibition can interfere with this process, which provides a potential therapeutic strategy to prevent early events of tissue damage-related innate immune cell activation and, ultimately, GVHD. (*Blood*. 2018;131(16):1858-1869)

Introduction

Allogeneic hematopoietic cell transplantation (allo-HCT) is a well-established treatment of a range of hematological diseases that cannot be cured by conventional chemotherapy.[1] More than 1 million HCTs have been performed globally to date, of which 40% were allogeneic.[2] The most common life-threatening complication after allo-HCT, and the primary factor limiting its success, is acute graft-versus-host disease (GVHD). The incidence of GVHD in allo-HCT remains high, despite immunosuppressive medication.[3] Overall, 60% of patients develop grade II to IV acute GVHD, 14% grade III to IV acute GVHD,[4] and 30% to 70% chronic GVHD.[5] The current concept of GVHD development is that antigen-presenting cells expressing foreign major histocompatibility complex (MHC) and minor histocompatibility antigens activate donor-derived T cells[3] in both lymphoid organs and target tissue.[6] The donor T cells expand and attack the recipient's tissues, mainly skin, liver, and gastrointestinal tract, leading to organ damage and dysfunction.[7] Most therapeutic regimens target the alloreactive T-cell activation and expansion, such as calcineurin inhibitors, antimetabolites (methotrexate and mycophenolate),[8] posttransplant cyclophosphamide,[9] or antithymocyte globulin.[10,11] Multiple groups have shown that in the early phase of GVHD before the expansion of alloreactive cytotoxic T cells, the irradiation or chemotherapy-based conditioning regimen lead to the activation of neutrophils,[12-14] monocytes,[15] and endothelial cells.[16,17]

These events are most likely not affected by the therapeutic strategies that target primarily T cells. In addition, it is also not known whether neutrophils ultimately contribute to the activation of the adaptive donor T-cell immune response against foreign (recipient) MHC or if local tissue damage is their only contribution to GVHD. The Janus Kinase (JAK) 1 and 2 inhibitor ruxolitinib has shown activity in reducing GVHD in the mouse model[18] and is currently under investigation in a phase 3 clinical trial for the treatment of steroid refractory GVHD (NCT02913482). In neutrophils, the JAK1 pathway is involved in granulocyte colony-stimulating-factor-mediated differentiation of neutrophils,[19] suggesting that neutrophil activation may require an intact JAK1 signaling.

In this study, we show that neutrophils do not homogeneously infiltrate the intestinal tract early after allo-HCT. Rather, they form clusters in the terminal ileum while absent from the colon. The ileum is the most exposed site for bacterial translocation, where neutrophils are recruited and then traffic into the mesenteric lymph nodes (mLNs), where they interact with and contribute to the activation of donor T cells. Antibody-based neutrophil depletion reduced donor T-cell expansion and acute GVHD severity.

JAK1/JAK2 inhibition by ruxolitinib reduced neutrophil numbers and MHC-II expression on neutrophils in the mLN. These findings indicate a novel role for neutrophils in mediating cellular communication between the damaged ileum and the mLN immediately after allo-HCT and provide a novel therapeutic option to interfere with early innate immune activation after conditioning-related tissue damage.

Materials and methods

Mice

C57BL/6 (H-2Kb, CD45.1 or CD45.2), BALB/c (H-2Kd, CD45.2), and FVB mice were purchased from Charles River Laboratory (Sulzburg, Germany), Janvier Labs (France), or the local stock of the animal facility at the University of Freiburg. C57BL/6 background Ptprc^{a} (B6.CD45.1^{+}, H-2^{b}, CD45.1^{+}) and B6D2F1 (H-2$^{b/d}$, CD45.2^{+}) were purchased from the Animal Resources Centre (Perth, WA, Australia), and subsequently were housed in sterilized microisolator cages and received acidified autoclaved water (pH 2.5) after transplantation. *Ccr2*$^{-/-}$ mice were provided by Marco Prinz (UKL Freiburg), *Tnf*$^{-/-}$ mice were provided by the Max Planck Institute of Immunobiology and Epigenetics (MPI Freiburg); *Alox5*$^{-/-}$ mice were also housed at the MPI Freiburg, and Dendra2 (B6;129S-*Gt(ROSA)26Sor*$^{tm1.1(CAG-COX8A/Dendra2)Dcc}$/J) mice[20] were housed at the UKL Würzburg. Transgenic mice were used only after genotyping. Mice were used between 6 and 14 weeks of age, and only female or male donor/recipient pairs were used. Animal protocols were approved by the Regierungspräsidium Freiburg, Freiburg, Germany (No: G15-018, G16-018 and G17/063) or approved by the institutional animal ethics committee (QIMR Berghofer, Australia).

Bone marrow transplantation model

Bone marrow (BM) transplantation experiments were performed as described.[13] The major mismatch strain combinations used were C57BL/6 into BALB/c, BALB/c into C57BL/6, FVB into BALB/c, or C57BL/6 into B6D2F1, as indicated in the respective experiments. Briefly, recipients were injected IV with 5×10^6 BM cells after lethal irradiation with 900 or 1100 cGy, split into 2 equal doses and 4 hours apart. To induce GVHD, CD4 and CD8 T cells were isolated from donor spleens and enriched by positive selection with the MACS cell separation system (Miltenyi Biotec, Germany), according to the manufacturer's instructions. Anti-CD4 and anti-CD8 MicroBeads were used. CD4^{+}/CD8^{+} T-cell purity was at least 90%, as assessed by flow cytometry. CD4^{+}/CD8^{+} T cells were given at a dosage of 0.3×10^6 to 1×10^7 IV on day 0, as indicated in the respective experiments. B6D2F1 mice (CD45.2^{+}) were lethally irradiated by 1100 cGy at 80.7 cGy/min, using a ^{137}Cs source 1 day before transplant. To induce GVHD, they were injected intravenously with 5×10^6 BM and 2×10^6 CD3^{+} T cells from B6.CD45.1^{+} mice.

Antibiotic treatment

An antibiotic cocktail consisting of vancomycin, metronidazole, cefoxitin, and gentamicin (final concentrations 1 mg/mL each) was added to the drinking water for 14 days before total body irradiation (TBI). Water bottles were changed every 2 to 3 days.

Aztreonam was dissolved in H2O, and mice received a subcutaneous injection of 75 mg/kg once daily for 7 days before and 1 day after TBI or H2O as solvent control.

Inhibitor treatment

Inhibitors, suppliers, concentration, diluent reagent, administration route, and treatment regimen is listed in supplemental Table 1, available on the *Blood* Web site.

Chemotherapeutic conditioning

Doxorubicin was dissolved in H2O and C57BL/6 mice received 20 mg/kg doxorubicin by intraperitoneal injection. Three days postinjection, mice were sacrificed and the white blood cell count was analyzed using an animal hematology analyzer (Scil Vet ABC). Ileum and mLN were processed for flow cytometric analysis as described earlier.

Quantitative polymerase chain reaction

Bacterial DNA from intestinal segments (0.5 cm long) was isolated after cutting the segments open longitudinally and removing feces by washing in phosphate-buffered saline. Epithelial layers were removed by washing in cell dissociation (CD) buffer (Hanks balanced salt solution without Mg^{2+}, Ca^{2+}, 5 mM EDTA, 10 mM *N*-2-hydroxyethylpiperazine-*N*′-2-ethanesulfonic acid) at 37°C for 15 minutes. The washing step was repeated 3 times. Bacterial and genomic DNA was isolated using the QIAamp cador Pathogen Mini Kit (Qiagen) according to the manufacturer's instructions, using pretreatment T2 for enzymatic digestion of tissue and pretreatment B1 for difficult-to-lyse bacteria.

DNA from stool samples for quantitation of the bacterial load was isolated using the stool QIAamp DNA Stool Mini Kit (Qiagen) according to the manufacturer's instructions.

Quantitative polymerase chain reaction was performed using the LightCycler 480 SYBR Green I Master Mix (Roche). Universal 16S primers (785F and 907R) were used for standardization of bacteria per tissue, and glyceraldehyde-3-phosphate dehydrogenase primers were used to determine levels of mouse genomic DNA, which was used as a reference (for primer sequences, see supplemental Table 2).

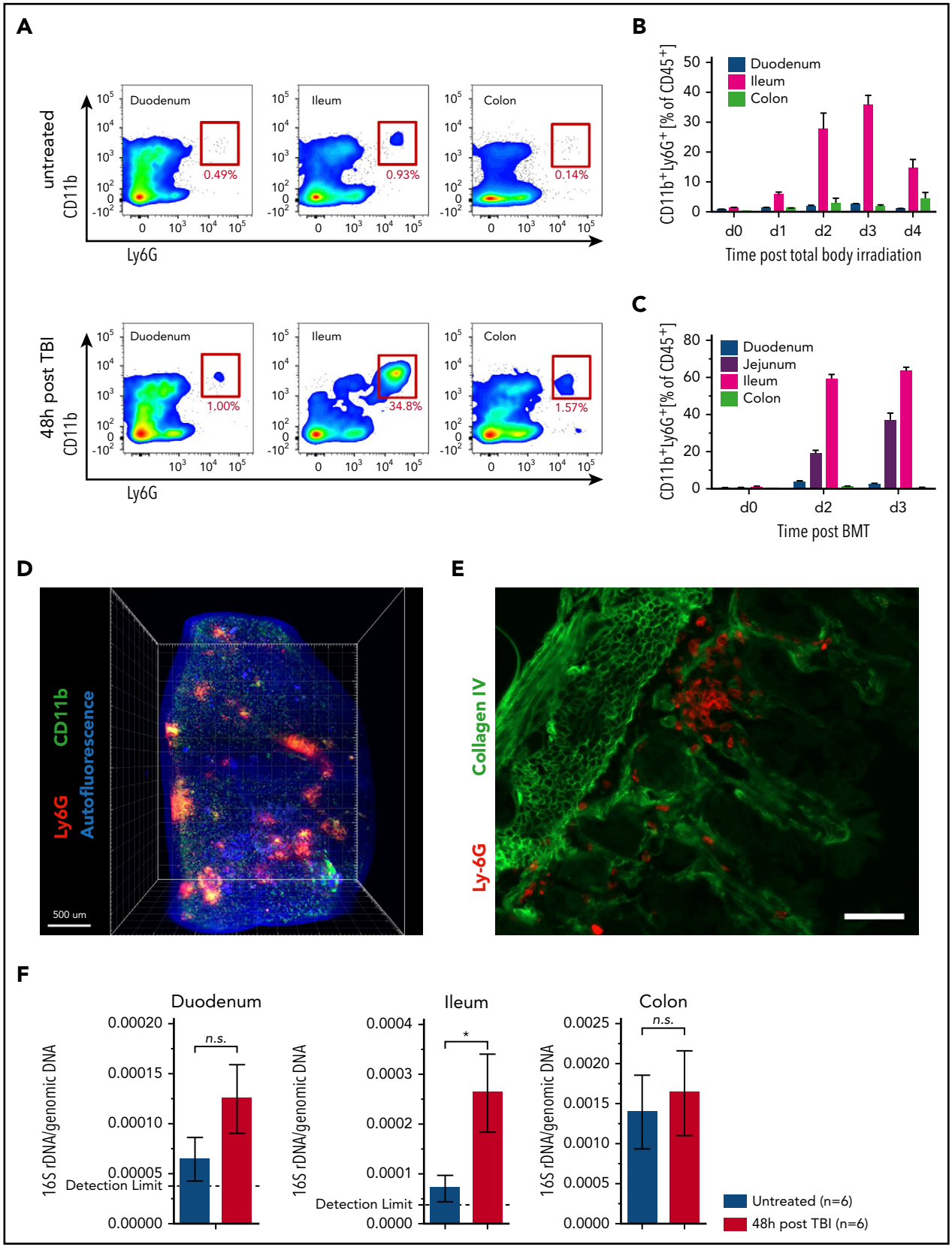

Figure 1. Neutrophil granulocytes selectively form clusters in the ileum after TBI. (A-B) Leukocytes were isolated from duodenum, ileum, and colon from untreated C57BL/6 mice, as well as after TBI, and analyzed by flow cytometry. Neutrophils are defined as viable $CD45^+CD11b^+Ly6G^+$ cells. (A) Representative plots of neutrophil numbers from untreated samples and 48 hours after TBI. (B) Pooled data from 2 separate experiments showing the percentages of $CD11b^+Ly6G^+$ cells of all leukocytes ($CD45^+$) at different points after TBI (n = 6-8). (C) C57BL/6 mice underwent allo-HCT (BALB/c into C57BL/6; 5×10^6 BM + 10^6 $CD4^+/CD8^+$ T cells). Leukocytes were isolated at different points after allo-HCT, and the percentages of $CD11b^+Ly6G^+$ cells of all leukocytes ($CD45^+$) are shown (n = 4). (D) Three-dimensional light sheet fluorescence microscopy of ileum 48 hours

Intestinal leukocyte isolation

Intestinal leukocytes were isolated as described.[21] In brief, 2- to 4-cm intestinal segments were dissected and Peyer's patches removed. Segments were opened longitudinally and rinsed in phosphate-buffered saline to remove feces. Epithelial cells were separated from the lamina propria using CD buffer (Hanks balanced salt solution without Mg^{2+}, Ca^{2+}, 5 mM EDTA, 10 mM *N*-2-hydroxyethylpiperazine-*N*′-2-ethanesulfonic acid), and the remaining tissue was digested with digestion buffer (Hanks balanced salt solution with Mg^{2+}, Ca^{2+}, collagenase D 0.5 mg/mL, DNAse 0.5 mg/mL, dispase 0.5 U/mL) to obtain single-cell suspensions that were further processed for flow cytometry.

Flow cytometry

Samples were washed in phosphate-buffered saline, and dead cells were stained using either Aqua LiveDead (Thermo Fisher) or Zombie NIR fixable dye (Biolegend). Fc receptors were blocked using anti-CD16/CD32, before staining with appropriate antibody concentrations for 30 minutes at 4°C. For a list of antibodies used, see supplemental Table 3. In some cases, cells were fixed in 0.5% paraformaldehyde. To calculate the absolute numbers of cells, a defined number of APC fluorescent beads (BD Bioscience) were added to the sample. Data were acquired within 2 hours after staining on a BD LSR Fortessa (BD Biosciences), and analysis was performed using FlowJo software (FlowJo, LLC).

Giemsa-Wright staining

Neutrophils ($CD45^+CD11b^+Ly6G^+$) were sorted on a FACS Aria III (BD Biosciences) into a 1.5-mL tube and prepared by cytospin at 47*g* for 5 minutes onto Superfrost Plus slides. Cells were fixed, permeabilized, and stained for 3 minutes in Giemsa Wright Solution (0.8 g Wright, 0.2 g Giemsa in methanol), followed by addition of an equal volume of phosphate buffer (pH 6.8) for 15 minutes.

Photoconversion of cells located in the terminal ileum

To selectively photoconvert cells in the terminal ileum of Dendra2 mice, the mice were anesthetized using ketamine-xylazine, and the abdomens surgically opened. The ileum was carefully mobilized using cotton swabs and a 2-cm segment of the ileum exposed to 405 nm light (405 nm Silver LED, Prizmatix; 0.5 NA polymer fiber with 1500 μm core diameter, Prizmatix; F671SMA-405 collimator, Thorlabs) for 7 minutes. This was done by moving the light a 0.2- to 0.5-cm distance alongside the ileum while the other body parts were shielded. For pain medication, the mice were treated with buprenorphine (0.1 mg/kg) intraperitoneally initially and at 0.01 mg/mL in the drinking water. Ten to 14 hours after surgery, mice were sacrificed and organs processed for fluorescence-activated cell sorter (FACS). Samples obtained from a sham-operated, nonilluminated mouse served as fluorescence minus 1 control for gating of photoconverted cells.

Statistical analysis

For statistical analysis, an unpaired *t* test (2-sided) was applied. If the data did not meet the criteria for normality, the Mann-Whitney *U* test was applied unless stated otherwise in the figure legend. Data are presented as mean and standard error of the mean (error bars). Differences were considered significant when the *P* value was $< .05$. *P* values are indicated as follows: $^*P < .05$; $^{**}P < .01$; $^{***}P < .001$.

All other methods are presented in the supplemental Methods.

Results

Neutrophil granulocytes form individual clusters in the ileum after TBI

In prior studies, we and others[12,13,22] have shown that recipient neutrophils infiltrate the intestinal tract after allo-HCT. However, the kinetics, anatomical localization, and responsible recruiting stimuli were undefined. We compared the duodenum, ileum, and colon on consecutive days after TBI and allo-HCT. We observed a selective increase of neutrophils in the terminal ileum that was severalfold higher than that of the duodenum or colon (Figure 1A-C). Absolute numbers of neutrophils increased in the ileum after TBI, while decreasing in other organs, including the spleen (supplemental Figure 1A-B). Infiltration of the ileum by neutrophils was not different when the mice underwent syngeneic or allogeneic HCT (supplemental Figure 1C). However, in the absence of allogeneic T cells, the mucosal injury exerted by the neutrophils in the syngeneic setting can heal, whereas in the allogeneic setting the neutrophil induced tissue damage promotes activation of allogeneic T cells and, as a secondary consequence, acute GVHD. Neutrophils accumulating in the ileum and mLN were mainly (99%) recipient derived (supplemental Figure 1D). The peak of neutrophil infiltration into the ileum was reached at 3 days after TBI and allo-HCT (Figure 1B). Neutrophils were not evenly distributed but accumulated in clusters (supplemental Figure 2A-B) that could be visualized by light sheet fluorescence microscopy and three-dimensional reconstruction of the ileum wall (Figure 1D; supplemental Video 1). $CD11b^+$ myeloid cells other than neutrophils did not form clusters (supplemental Video 2). Closer analysis revealed that neutrophils selectively accumulated at the bottom of the crypts (Figure 1E) in close proximity to the lymphatic vessels of the ileum (supplemental Video 3).

To test for stimuli released early after TBI conditioning, we analyzed changes in cytokine expression in ileum and colon 24 hours after TBI (supplemental Figure 3A). Although there was a pronounced change in the ileal cytokine expression profile (12 cytokines $>1.5\times$ upregulated), there were only minor changes in the colon (1 cytokine $>1.5\times$ upregulated), indicating that the ileum is more susceptible to TBI (supplemental Figure 3B). As expected, the myeloperoxidase that is strongly expressed in neutrophils was highly upregulated in the ileum. Chemoattractants that have been reported to be involved in neutrophil attraction, including CXCL1, CXCL2, CXCL5, and IL-17A, did not increase after TBI (supplemental Figure 3C). CD160, a glycoprotein mainly expressed on intraepithelial lymphocytes,

Figure 1 (continued) after TBI showed cluster formation of neutrophils (Ly6G, red; CD11b, green; tissue autofluorescence, blue). (E) Immunofluorescence staining of ileal cross-section 48 hours after TBI showed localization of neutrophils adjacent to intestinal crypts (Collagen IV, green; Ly6G, red; scale bar, 50 μm). (F) Bacterial load in lamina propria of duodenum, ileum, and colon of untreated C57BL/6 mice and C57BL/6 mice 48 hours after TBI was analyzed by quantitative reverse transcription-polymerase chain reaction. 16S rDNA content was normalized to mouse genomic DNA (glyceraldehyde-3-phosphate dehydrogenase). Pooled data from 2 individual experiments are shown (n = 6).

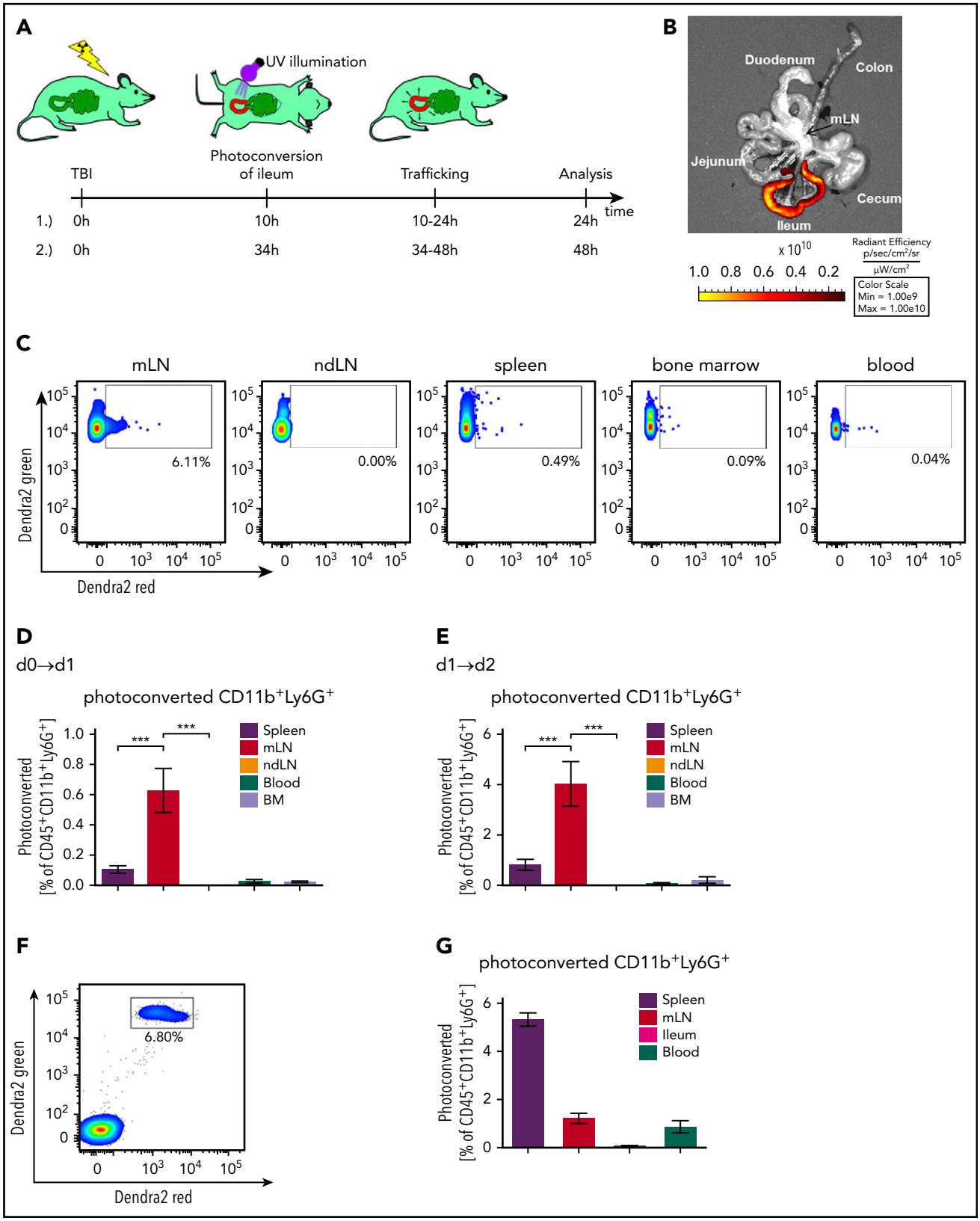

Figure 2. Neutrophils migrate from the ileum to the mesenteric lymph node. Mice transgenic for the photoconvertible green-to-red protein Dendra2 in all cells underwent TBI. After 10 or 34 hours, the ileum was exposed to 405-nm light during surgery to convert Dendra2 from its green to the red fluorescent form. Mice were sacrificed 10-14 hours after illumination and the amount of photoconverted cells that had trafficked from ileum to spleen, mLN, ndLN (nondraining lymph node, pooled iLN and aLN), blood, and BM was determined. (A) Illustration of experimental setup. (B) Representative fluorescence image showing successful photoconversion selectively in the ileum after surgery. (C) Representative FACS plots of photoconverted $CD45^+CD11b^+Ly6G^+$ cells 48 hours after TBI in different organs. Pixel size of dots was increased for better visibility. (D-E) Percentage of photoconverted $CD11b^+Ly6G^+$ neutrophils is shown. (D) Photoconversion on day 0, 10 hours post-TBI, and analysis on day 1, 24 hours post-TBI, according

showed the highest change in expression in the ileum (supplemental Figure 3B). When analyzing for CD160$^+$ cells by flow cytometry, we observed high abundance of CD160$^+$ cells in the epithelial layer, whereas only few cells resided in the lamina propria. However, CD160$^+$ cells did not increase in numbers (supplemental Figure 3D) after TBI.

To investigate the role of other stimuli potentially attracting neutrophils to the ileum wall, we used mice genetically lacking tumor necrosis factor, CCR2, or 5-Lipoxygenase (*Alox5*$^{-/-}$) as recipients. These molecules were chosen on the basis of reports indicating their roles in neutrophil chemotaxis in other situations of an innate immune response.[23-25] We found unaltered neutrophil infiltration into the ileum in the individual absence of any of these molecules (supplemental Figure 3E), indicating that individually they are not necessary for neutrophil recruitment to the ileum during the early phase of GVHD.

By using pharmacological inhibitors, we could also exclude the involvement of other factors known to play a role in myeloid cell chemotaxis, including sphingosine-phosphate 1 receptor, CXCR2, TLR4, and PI3K (supplemental Figure 3F). In addition, butyrate, which has been shown to be protective for the intestinal wall during GVHD,[26] had no effect on neutrophil recruitment (supplemental Figure 3F). These findings indicate a strictly time- and location-dependent influx of neutrophils into the terminal ileum after allo-HCT, which is independent of several of the previously described stimuli driving myeloid cell chemotaxis in other disease models.

We hypothesized that the difference in neutrophil recruitment reflected differential translocation of bacteria into the intestinal wall in the various sections of the gut. Therefore, we analyzed the different intestinal regions with respect to the presence of bacterial 16S rDNA in the bowel wall. The increase of bacterial 16S rDNA in the ileal wall on TBI was substantial and significant. In the duodenum and the colon wall, in contrast, there was almost no increase in bacterial DNA detectable (Figure 1F), supporting the concept that the translocation of bacteria is responsible for the early infiltration of neutrophils specifically into the ileum after allo-HCT, and that this translocation is the variable that determines the initiation of GVHD in the ileum. By sequencing the translocating bacteria in the lamina propria of the ileum before and after TBI, we observed that *Clostridiales* species were enriched, whereas the abundance of *Bdellovibrionales* and *Desulfovibrio* was decreased (supplemental Figure 4A).

Neutrophils migrate from the ileum to the mLN

Dendritic cells (DCs) traffic from the intestinal tract to secondary lymphoid organs to participate in T-cell activation in GVHD.[27] To understand whether neutrophils that have been activated in the intestinal tract later migrate to mLN, we used mice transgenic for the Dendra2 protein,[20] a photoconvertable fluorescent protein that undergoes an irreversible emission shift from green to red fluorescence on illumination with 405-nm light (Figure 2A).

We observed successful conversion of the Dendra2 protein in neutrophils when the ileum was selectively illuminated in a surgical procedure (Figure 2B; supplemental Figure 5A-B). The ileum was then placed back in the abdominal cavity, and the abdomen was surgically closed. After 10 to 14 hours, lymphoid organs were analyzed for the presence of red Dendra2-positive cells. To better evaluate neutrophil migration kinetics, we analyzed the frequency of photoconverted neutrophils on day 1 and day 2 after TBI, in both cases 10 to 14 hours after the ileum had been exposed to 405-nm light. We detected the highest frequency of photo-converted ileum-derived neutrophils in the mLN, which drains the ileum (Figure 2C-E; supplemental Figure 5C). In contrast to these endogenous neutrophils recruited via the lymphatic system from the ileum to the mLN, exogenous BM-derived neutrophils injected intravenously accumulated mainly in the spleens of the recipients (Figure 2F-G). A sham-operated, nonilluminated mouse served as fluorescence minus 1 control for correct gating of photoconverted cells (supplemental Figure 5C). In addition to neutrophils, CD11c$^+$ DCs also were found to migrate from the ileum to the mLN (supplemental Figure 5D). These findings provide evidence that neutrophils migrate from the ileum to the mLN after TBI.

Neutrophils translocate to the mesenteric lymph nodes mediating cellular communication between the tissue injury site and the secondary lymphoid organ

Tissue damage translates into GVHD when alloreactive T cells are activated by the release of cytokines and enhanced antigen presentation by antigen-presenting cells. Our data show that neutrophils migrate from the damaged intestinal tract to the mLN, where some T-cell priming takes place. We next validated this finding by analyzing the neutrophil counts in lymphoid organs after irradiation. We detected increased neutrophil numbers in the mLN, but not in inguinal (iLN) or axillary (aLN) lymph nodes or in the spleen (Figure 3A).

Similarly, DCs also infiltrated the mLN (supplemental Figure 6A); however, the relative increase of neutrophils was higher. mLN-derived CD45$^+$CD11b$^+$Ly6G$^+$ cells, isolated by cell sorting, showed neutrophil-typical hypersegmented morphology (Figure 3B). In individual mice, there was a positive correlation between neutrophil infiltration in the ileum and in the mLN, which provided additional evidence that neutrophils infiltrating the ileum moved on to its draining lymph nodes (Figure 3C).

To understand whether bacterial translocation through the ileum translated into increased appearance of bacterial components in the mLN, we determined 16S rDNA in that organ. Copies of 16S rDNA were significantly increased in the mLN at 48 hours after TBI compared with untreated mice (Figure 3D); this finding was

Figure 2 (continued) to setup A1 (n = 6 for each organ from 2 independent experiments). (E) Photoconversion on day 1, 34 hours post-TBI, and analysis on day 2, 48 hours after TBI according to setup A2 (n = 7 for each organ from 2 independent experiments). (F-G) Neutrophils from the BM of mice transgenic for the photoconvertible green-to-red fluorescence protein Dendra2 were isolated and enriched by MACS purification. The cells were photoconverted ex vivo, and 10^7 neutrophils were adoptively transferred into C57BL/6 mice 34 hours after they underwent TBI. Fourteen hours after injection and 48 hours after TBI, mice were sacrificed, and photoconverted Dendra2 cells in spleen, mLN, ileum, and blood was analyzed by flow cytometry. (F) Representative FACS plots of photoconverted CD45$^+$CD11b$^+$Ly6G$^+$ cells derived from the spleen. (G) Percentage of photoconverted CD11b$^+$Ly6G$^+$ neutrophils in different organs is shown (n = 8).

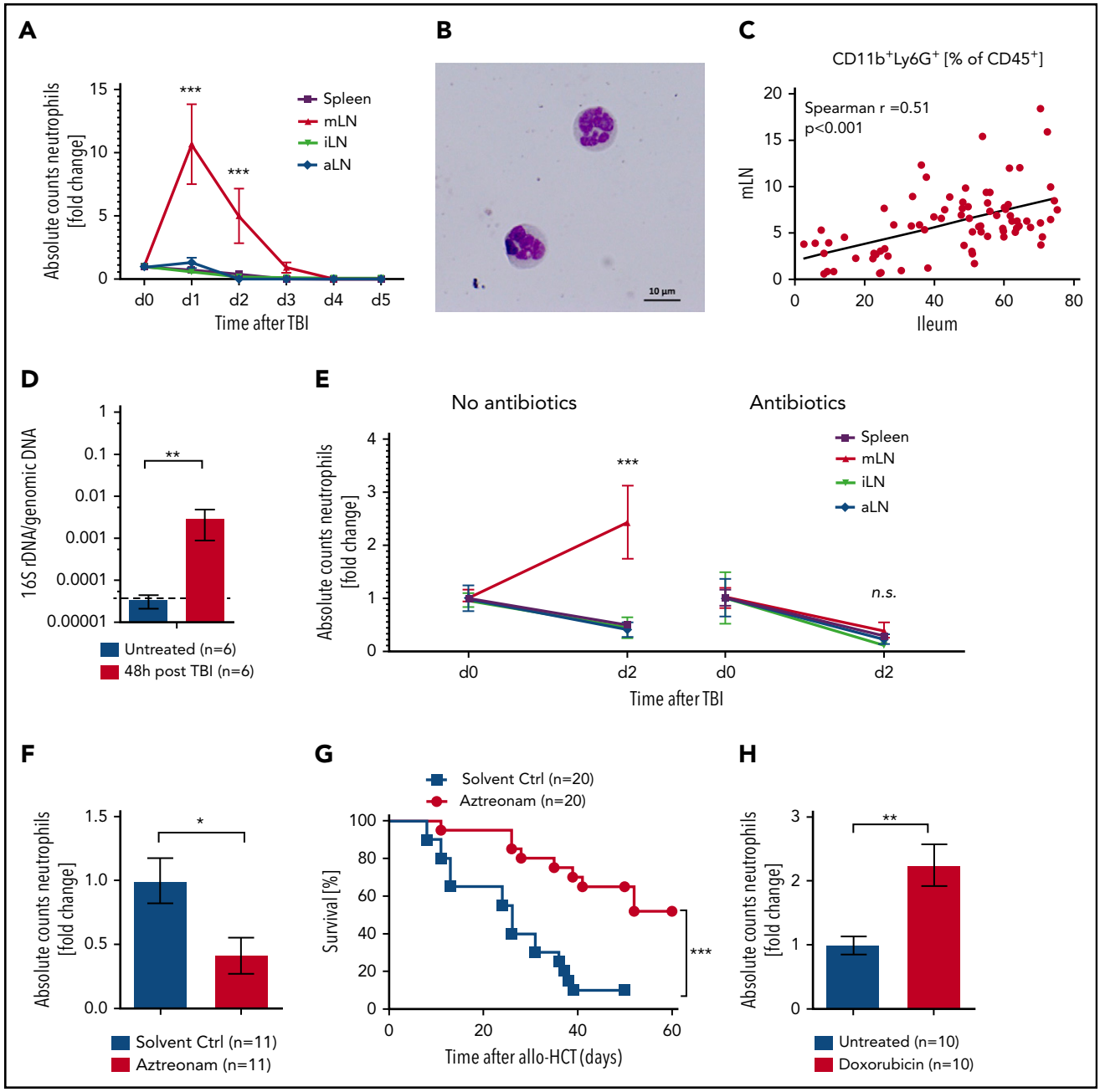

Figure 3. Neutrophil infiltration in lymphatic organs. (A) Neutrophil counts in spleen, mLN, iLN, and aLN at different points after TBI were analyzed by flow cytometry. Fold change of absolute numbers with regard to untreated mice (day 0) is presented (n = 6 for each point and organ from 2 independent experiments). (B) Giemsa-Wright staining of mLN-derived $CD45^+CD11b^+Ly6G^+$ neutrophils after FACS sorting and cytospin. (C) Correlation of neutrophil frequency in mLN and ileum from WT or solvent control-treated mice (n = 57). (D) Bacterial load in mLN of untreated C57BL/6 and 48 hours after TBI were analyzed by quantitative reverse transcription-polymerase chain reaction. 16S rDNA content was normalized to genomic DNA (glyceraldehyde-3-phosphate dehydrogenase). (E) Fold change of neutrophil numbers on day 2 after TBI normalized day o d0 (no TBI) in C57BL/6 mice with and without gut decontamination is shown (Control treatment, n = 10; gut decontamination, n = 6 each point and organ from 2-3 independent experiments). (F) C57BL/6 mice were treated daily by subcutaneous injection of aztreonam (75 mg/kg/d) or solvent control from day −7 until day +1 and underwent TBI on day 0. Fold change of neutrophil numbers on day 2 post TBI normalized to mean of solvent controls is shown (n = 11 pooled from 2 independent experiments). (G) BALB/c mice were treated daily by subcutaneous injection of aztreonam (75mg/kg/day) or solvent control from day −7 until day +1 and received allo-HCT (C57BL/6 into BALB/c; 5×10^6 BM cells + 0.3×10^6 $CD4^+/CD8^+$ T cells) on day 0, and survival was monitored (n = 20 for each group pooled from 2 independent experiments). (H) C57BL/6 mice received 20 mg/kg doxorubicin on day 0 or were left untreated. The mLN were analyzed on day 3 by flow cytometry to assess neutrophils counts ($CD45^+CD11b^+Ly6G^+$). Fold change of neutrophil numbers normalized to the mean of untreated samples is shown (n = 10 for each group pooled from 2 independent experiments).

confirmed by sequence analysis (supplemental Figure 6B). We hypothesized that the influx of bacteria or their constituents into the mLN would attract neutrophils, which led us to study their presence under various conditions. The increased infiltration of the mLN by neutrophils was abrogated when the mice had been treated with antibiotics before TBI (Figure 3E), underlining the dependence of neutrophil migration on the presence of bacteria. This antibiotic treatment reduced the bacterial load in the

feces by 45 000 times (supplemental Figure 6C), which is different from the broad-spectrum antibiotics given to patients after allo-HCT that do not aim at completely eliminating all bacteria. Treatment with aztreonam reduced neutrophil recruitment to the ileum (supplemental Figure 6D) and mLN (Figure 3F) and GVHD-related death compared with the vehicle control group (Figure 3G). In addition, we analyzed the effect of doxorubicin on neutrophil recruitment to the intestinal tract. We observed that at day 3 postdoxorubicin administration, when the white blood count in the peripheral blood was decreased (supplemental Figure 6E), the frequency of neutrophils was still increased in the ileum (supplemental Figure 6F) and the mLN (Figure 3H) compared with untreated mice.

Neutrophils in the mesenteric lymph node and ileum express high levels of MHC-II and contribute to the expansion of donor T cells

To better understand whether the neutrophils that had migrated from the ileum to the mLN in a bacteria-dependent manner would interact with donor-derived T cells, we analyzed interactions of neutrophils and T cells in the mLN. We observed an accumulation of neutrophils around the T-cell zone in close proximity to lymphatic vessels (Figure 4A) and a frequent colocalization of neutrophils with donor type (CD45.1$^+$) T cells (Figure 4B).

Neutrophils are not considered classical antigen-presenting cells. However, several reports have indicated that activated neutrophils can express MHC II and can indeed effectively present antigen to T cells.[28] We hypothesized that such interaction between neutrophils and T cells may take place after TBI and next determined the MHC-II levels of neutrophils derived from spleen, mLN, iLN, aLN, or ileum, after irradiation. We found a significantly greater proportion of MHC-II expressing neutrophils in the ileum and mLN compared with neutrophils residing in nondraining lymph nodes or the spleen (Figure 4C-D).

To determine whether neutrophils can present host antigens in a recipient MHC-II-dependent manner and whether they increase their presentation capacity after TBI, we used a previously described system using the YAe antibody. This antibody stains the complex of Ea peptide (I-A^d derived from DBA/2) bound to I-A^b (expressed on C57BL/6).[29] Recipient mice (B6D2F1) were the F1 generation of C57BL/6 and DBA/2 mice, and therefore expressed DBA/2 MHC-II (I-A^d). We observed that a proportion of neutrophils was indeed presenting Ea peptide in the context of MHC-II (Figure 4E). Both the percentage and the absolute numbers of YAe$^+$/MHC-II$^+$ neutrophils present in the mLN increased by 48 hours after BM transplantation compared with untreated mice (Figure 4F), indicating the enhanced ability of these neutrophils to participate in antigen presentation to donor T cells. Indeed, depletion of neutrophils with anti-Ly6G antibodies caused a small but statistically significant reduction in CD4 T-cell proliferation in the mLN (Figure 4G-H). Decreased T-cell expansion in mice treated with anti-Ly6G antibody was not a result of decreased MHC-II or CD80/86 expression on DCs, as these markers were even increased on DCs after anti-Ly6G Ab treatment (supplemental Figure 7A-B). Anti-Ly6G antibody treatment reduced GVHD-related death at 2 different T-cell dosages (Figure 4I; supplemental Figure 7C).

Ruxolitinib treatment reduces numbers of neutrophils in the mLN as well as their MHC-II expression

Small-molecule kinase inhibitors have shown great potential for the therapeutic interference with signaling pathways in both cancer and immune cells. Ruxolitinib is a JAK1/JAK2 inhibitor that can reduce GVHD in preclinical models. To test whether JAK1/JAK2 are involved in neutrophil migration and activation during GVHD, we treated mice with the ruxolitinib twice daily and analyzed neutrophil numbers in ileum and mLN, together with MHC-II and CD80/CD86 levels on these cells. Mice treated with ruxolitinib had lower absolute numbers of leukocytes and of neutrophils in the mLN, whereas no significant changes were observed in the ileum (supplemental Figure 8A; Figure 5A).

Although CD80/86 expression remained unchanged (supplemental Figure 8B), the frequency of MHC-II$^+$ neutrophils 48 hours after TBI in the ileum and mLN was reduced in ruxolitinib-treated mice compared with control irradiated mice (Figure 5B-C). In addition, the neutrophils that did migrate to the mLN in ruxolitinib-treated mice showed lower MHC-II expression compared with vehicle-treated mice (Figure 5D-E).

The numbers of MHC-II$^+$ neutrophils in the mLN were positively correlated with the numbers of MHC-II$^+$ neutrophils in the ileum in mice undergoing TBI and vehicle treatment (Figure 5F). This correlation was not seen when mice had been treated with ruxolitinib (Figure 5F). This indicates that despite infiltration of the ileum, neutrophil trafficking from the ileum to mLN is disrupted by treatment with ruxolitinib. In summary, these results show that ruxolitinib treatment can reduce neutrophil numbers in the mLN and inhibit their ability to stimulate T cells in the mLN resulting from lower MHC-II expression.

Discussion

Early events of GVHD include the release of damage-associated molecular patterns[30-32] and the activation of Ag-presenting cells that later prime donor T cells. A recent study has shown that when GVHD is established, donor CD103$^+$ DCs that were stimulated by damage-associated molecular patterns/pathogen-associated molecular patterns then migrate from the colon to the mLN and provide a feed-forward loop to amplify GVHD.[27] In the study presented here, we analyzed events that precede established GVHD and found that after TBI, the terminal ileum is the most vulnerable site to intestinal leakage, leading to the most abundant infiltration by neutrophils. Although the ileum is far less densely colonized by bacteria than the colon, both bacterial rDNA and bacteria-dependent neutrophil infiltration were much more pronounced in the ileum wall compared with the colon. By using a photoconverter in vivo system, we could show that neutrophils that had been converted in the ileum later appeared in the mLN. Colocalization of neutrophils and donor T cells in the mLN was observed, and functional studies revealed reduced CD4 T-cell expansion when neutrophils were reduced by antibody-mediated depletion. In addition to direct T-cell priming, it is likely that neutrophils affect T-cell expansion indirectly via increased inflammation resulting from tissue damage in the ileum.

Translocated bacteria are essential for the neutrophil migration. When using antibiotics-based decontamination before TBI, we

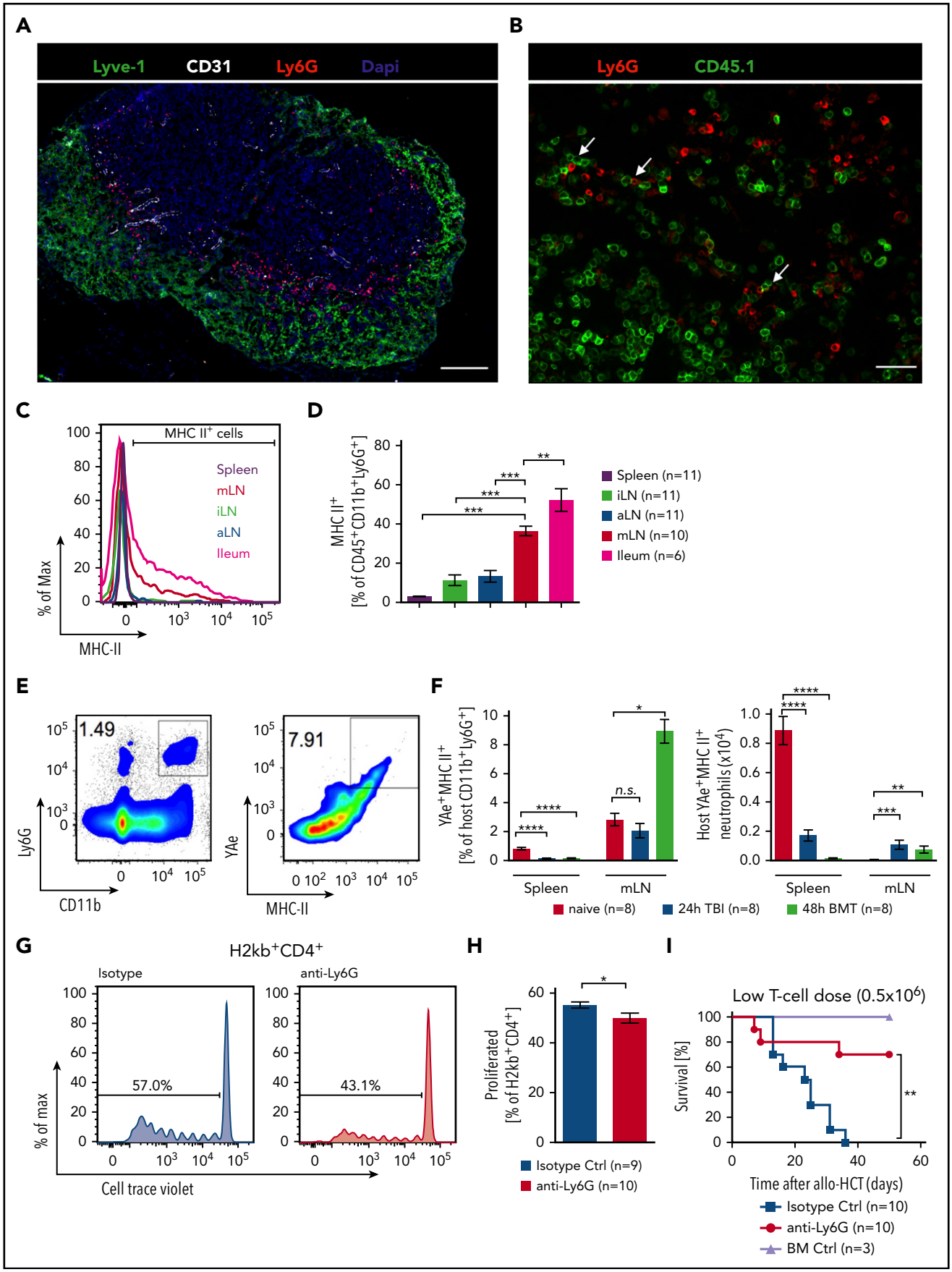

Figure 4.

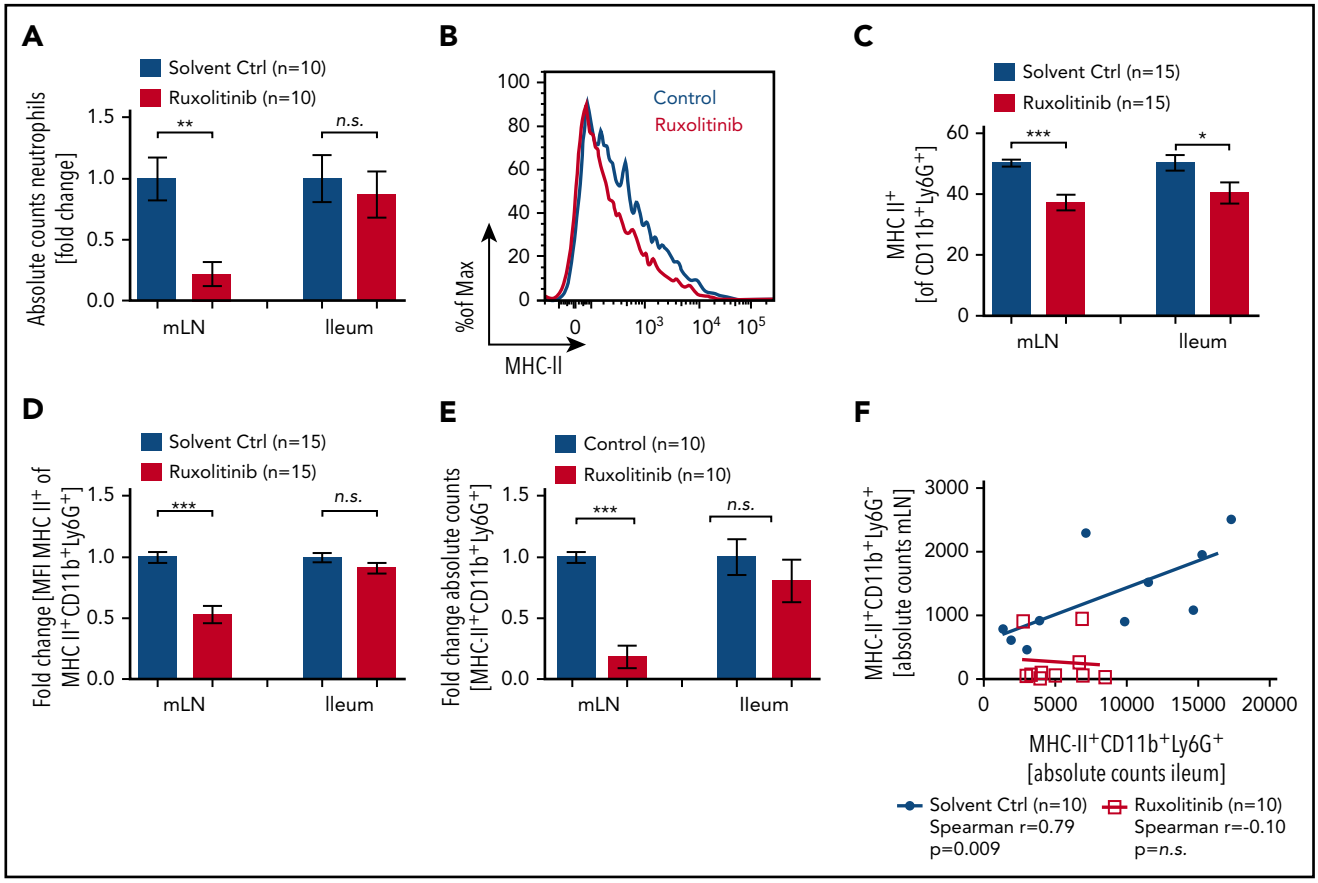

Figure 5. JAK1/JAK2 inhibition reduces neutrophils and MHC-II expression. C57BL/6 mice were treated twice daily with 30 mg/kg ruxolitinib starting on day −1 before TBI. On day 2 after TBI, mice were sacrificed and analyzed by flow cytometry. (A) Absolute numbers of neutrophils ($CD45^+CD11b^+Ly6G^+$) in mLN and ileum. (B) Representative histogram of MHC-II expression on $CD45^+CD11b^+Ly6G^+$ neutrophils in ileum after ruxolitinib or solvent control treatment. (C) Frequency of MHC-II^+ (% of $CD45^+CD11b^+Ly6G^+$) neutrophils in ileum and mLN after ruxolitinib or solvent control treatment. (D) Fold change of MFI for MHC-II on MHC-$II^+CD11b^+Ly6G^+$ cells isolated from mLN or ileum. (E) Fold change in absolute MHC-$II^+CD45^+CD11b^+Ly6G^+$ numbers by ruxolitinib treatment normalized to solvent control. (F) Correlation of MHC-$II^+CD45^+CD11b^+Ly6G^+$ neutrophil numbers in mLN vs ileum after ruxolitinib or solvent control treatment.

found no trafficking to the mLN. Depletion of neutrophils resulted in reduced CD4 T-cell proliferation and reduced GVHD severity. These observations indicate that both phenomena, translocated bacteria and intestinal neutrophil accumulation, are connected and play a role in GVHD. Although neutrophils are classically thought to express low cell-surface levels of MHC-II, we observed high levels for mLN or ileum-derived neutrophils after TBI. Consistent with these findings, neutrophils have been found to be able to prime T cells in vitro,[28] in a colitis model,[33,34] and in a skin injury model.[35] These reports are in agreement with our observation that neutrophils in the mLN migrated there from the ileum and presented recipient antigen to donor T cells. Our finding that neutrophil depletion reduces GVHD-related death indicates a role of neutrophils in GVHD. However, how pivotal the role is under different clinical conditions, such as reduced intensity conditioning, has still to be determined.

Beyond the novel biological observation that neutrophils contribute to T-cell priming, we also provide evidence of the potential usefulness of a therapeutic intervention that may allow countering early innate immune activation after tissue damage. We observed that the JAK1/JAK2 inhibitor ruxolitinib reduced the stimulatory capacity of neutrophils by reducing their MHC-II expression. In addition, ruxolitinib treatment reduced the

Figure 4. Antigen presentation by neutrophils. (A) Immunofluorescence staining of a mLN 48 hours after TBI showing ring-shaped localization of $Ly6G^+$ cells (red) around lymphocytes next to lymphatic vessels (Lyve-1, green; 4′,6-diamidino-2-phenylindole, blue; blood vessels (CD31), white; scale bar, 200 μm). (B) MLN 48 hours after allo-HSCT showing neutrophils ($Ly6G^+$ = red) close to transplanted CD45.1$^+$ T cells (green, scale bar = 150 μm). (C) Representative histogram of MHC-II expressing $CD45^+CD11b^+Ly6G^+$ neutrophils in spleen, iLN, aLN, mLN, and ileum in C57BL/6 mice 48 hours after TBI. (D) Frequency of MHC-II^+ (percentage of $CD45^+CD11b^+Ly6G^+$) neutrophils in different organs in CD57Bl/6 mice 48 hours after TBI. (E-F) MHC-II expression and peptide presentation (YAe^+) on $CD11b^+Ly6G^+$ neutrophils in B6D2F1 mice were assessed by flow cytometry in untreated mice, 24 hours after TBI and 48 hours after BM transplantation. (E) Representative FACS plots showing gating strategy. (F, left) Relative numbers of YAe^+MHC-II^+ cells of host neutrophils. (Right) Absolute numbers of host YAe^+MHC-II^+ neutrophils. (G-H) For neutrophil depletion, BALB/c mice were injected with either anti-Ly6G (0.5 mg intraperitoneally) or an isotype control (0.5 mg) on day −1 and transplanted after TBI on day 0 with 1×10^7 purified and CellTrace Violet-labeled $CD4^+/CD8^+$ T cells from C57BL/6 mice. Mice were sacrificed on day 3 and mLN analyzed for donor-derived ($H2kb^+$) T cells that had proliferated. (G) Representative flow cytometry plots of CellTrace Violet-dilution of $H2kb^+CD4^+$ T cells. (H) Pooled data from 2 independent experiments showing proliferated $H2kb^+CD4^+$ T cells after anti-Ly6G neutrophils depletion. (I) BALB/c mice were treated on day −1 by anti-Ly6G (0.5 mg) or isotype control antibody (0.5 mg) injection and underwent allo-HCT (FVB into BALB/c; 5×10^6 BM cells + 0.5×10^6 $CD4^+/CD8^+$ T cells). BM controls were treated on day 0 by isotype control antibody (0.5 mg) injection and underwent transplantation using BM alone (FVB 5×10^6 cells).

number of neutrophils in the mLN. Intriguingly, neutrophils were still able to migrate to the ileum but were prevented from moving on to the mLN. It is clear that DCs play an important role in the stimulation of T cells in GVHD, and our data presented here suggest that neutrophils also play a role in direct T-cell activation, and that ruxolitinib also affects the T-cell-stimulating function of neutrophils. These findings are consistent with our previous findings showing that the JAK/STAT/MHC-II axis in DCs can be blocked by ruxolitinib.[36] Thus, ruxolitinib acts on both types of APCs, and thereby interferes with major events of early GVHD. A next step could be to bring early JAK1/JAK2 inhibition in the clinic as a prophylactic, rather than only therapeutic, strategy. By reducing the contribution of neutrophils to early events in GVHD pathophysiology, one could potentially improve the outcome of patients undergoing allo-HCT.

In summary, we provide a characterization of the pathomechanistic chain of bacterial transmigration into the ileum wall, subsequent neutrophil recruitment, neutrophil migration into the draining lymph node, presentation of host-derived antigen by neutrophils, and consecutively increased donor T-cell expansion. Our findings improve our understanding of the early pathogenic steps of GVHD and identify a contribution of neutrophils to the adaptive allogeneic immune response. In addition, we were able to interfere therapeutically with the process by JAK1/JAK2 inhibition through ruxolitinib, reducing the accumulation of neutrophils and DCs in the mLN, as well as reducing MHC-II expression of these cell types. This offers a rational explanation of the use of kinase inhibitors as a potential therapeutic option, to inhibit antigen-presentation after conditioning induced tissue damage, an early step in the initiation of GVHD.

Acknowledgments

The authors thank the staff of the Life Imaging Center in the Center for Biological Systems Analysis of the Albert-Ludwigs-University Freiburg and the Core Facility of the University Medical Center Freiburg for help with their confocal microscopy and flow cytometry resources. The authors further thank Gabriele Niedermann and Simone Gaedicke for providing the irradiation source for certain animals.

This study was supported by the Deutsche Forschungsgemeinschaft, Germany, SFB1160, project P14, ZE 872/4-1 (R.Z.), TRR167-NeuroMAC (R.Z.), ERC Consolidator grant (681012 GvHDCure) (R.Z.), Wilhelm Sander Stiftung (grant 2008.046.4), and Deutsche Krebshilfe (No. 111639) (R.Z. and G.H.), and from the National Institutes of Health, National Institute of Allergy and Infectious Diseases (U01 AI22285) (M.J.B.) and National Institutes of Health, National Heart, Lung, and Blood Institute (R01 HL56067) (B.R.B.), and the C & D Fund (M.J.B). This study was also supported in part by the Excellence Initiative of the German Research Foundation (GSC-4, Spemann Graduate School).

Authorship

Contribution: J.H. helped develop the concept, performed experiments, analyzed data, and helped write the manuscript; K.J.O. helped perform light sheet fluorescence imaging, set up Dendra2 photoconversion, and analyzed data; H.P.N. helped perform mouse surgery experiments; M.K. performed experiments and analyzed data; Z.G. performed microbiota analysis; O.S.T., A.A.-A., G.P., S.D., H.D., and S.K. performed experiments; T.L. provided vital reagents and helped plan experiments; M.J.B. helped analyze the microbiome data and helped with the experimental planning and manuscript preparation; B.T.F. and B.R.B. helped design experiments; A.B. and G.R.H. helped plan experiments, analyzed data, and helped write the manuscript; G.H. helped develop the concept, plan and analyze the experiments, and write the manuscript; R.Z. designed the study, supervised the experiments, analyzed data, and wrote the manuscript.

Conflict-of-interest disclosure: The authors declare no competing financial interests.

Correspondence: Robert Zeiser, Department of Hematology, Oncology and Stem Cell Transplantation, University Medical Center Freiburg, Freiburg, D-79106 Freiburg, Germany; e-mail: robert.zeiser@uniklinik-freiburg.de.

Footnotes

Submitted 24 October 2017; accepted 9 February 2018. Prepublished online as *Blood* First Edition paper, 20 February 2018; DOI 10.1182/blood-2017-10-812891.

*G.H. and R.Z. co-supervised the work.

The online version of this article contains a data supplement.

There is a *Blood* Commentary on this article in this issue.

The publication costs of this article were defrayed in part by page charge payment. Therefore, and solely to indicate this fact, this article is hereby marked "advertisement" in accordance with 18 USC section 1734.

REFERENCES

1. Forman SJ, Negrin RS, Antin JH, Appelbaum FR, eds. Thomas' Hematopoietic Cell Transplantation. 5th ed. Hoboken, NJ: Wiley-Blackwell; 2016.
2. Gratwohl A, Pasquini MC, Aljurf M, et al; Worldwide Network for Blood and Marrow Transplantation (WBMT). One million haemopoietic stem-cell transplants: a retrospective observational study. *Lancet Haematol.* 2015;2(3):e91-e100.
3. Zeiser R, Blazar BR. Acute Graft-versus-host disease - Biologic process, prevention, and therapy. *N Engl J Med.* 2017;377(22):2167-2179.
4. Pasquini MC, Zhu X. Current use and outcome of hematopoietic stem cell transplantation. Milwaukee, WI: 2015 CIBMTR Summary Slides; 2014.
5. Arai S, Arora M, Wang T, et al; Graft-vs-Host Disease Working Committee of the CIBMTR. Increasing incidence of chronic graft-versus-host disease in allogeneic transplantation: a report from the Center for International Blood and Marrow Transplant Research. *Biol Blood Marrow Transplant.* 2015;21(2):266-274.
6. Koyama M, Hill GR. Alloantigen presentation and graft-versus-host disease: fuel for the fire. *Blood.* 2016;127(24):2963-2970.
7. Blazar BR, Murphy WJ, Abedi M. Advances in graft-versus-host disease biology and therapy. *Nat Rev Immunol.* 2012;12(6):443-458.
8. Storb R, Deeg HJ, Whitehead J, et al. Methotrexate and cyclosporine compared with cyclosporine alone for prophylaxis of acute graft versus host disease after marrow transplantation for leukemia. *N Engl J Med.* 1986;314(12):729-735.
9. Kanakry CG, Tsai HL, Bolaños-Meade J, et al. Single-agent GVHD prophylaxis with post-transplantation cyclophosphamide after myeloablative, HLA-matched BMT for AML, ALL, and MDS. *Blood.* 2014;124(25):3817-3827.
10. Finke J, Bethge WA, Schmoor C, et al; ATG-Fresenius Trial Group. Standard graft-versus-host disease prophylaxis with or without anti-T-cell globulin in haematopoietic cell transplantation from matched unrelated donors: a randomised, open-label, multicentre phase 3 trial. *Lancet Oncol.* 2009;10(9):855-864.
11. Kröger N, Solano C, Wolschke C, et al. Antilymphocyte Globulin for Prevention of Chronic Graft-versus-Host Disease. *N Engl J Med.* 2016;374(1):43-53.
12. Socié G, Mary JY, Lemann M, et al. Prognostic value of apoptotic cells and infiltrating neutrophils in graft-versus-host disease of the

gastrointestinal tract in humans: TNF and Fas expression. *Blood*. 2004;103(1):50-57.

13. Schwab L, Goroncy L, Palaniyandi S, et al. Neutrophil granulocytes recruited upon translocation of intestinal bacteria enhance graft-versus-host disease via tissue damage. *Nat Med*. 2014;20(6):648-654

14. Fischer JC, Wintges A, Haas T, Poeck H. Assessment of mucosal integrity by quantifying neutrophil granulocyte influx in murine models of acute intestinal injury. *Cell Immunol*. 2017;316:70-76.

15. Klämbt V, Wohlfeil SA, Schwab L, et al. A novel function for P2Y2 in myeloid recipient–derived cells during graft-versus-host disease. *J Immunol*. 2015;195(12):5795-5804.

16. Leonhardt F, Grundmann S, Behe M, et al. Inflammatory neovascularization during graft-versus-host disease is regulated by αv integrin and miR-100. *Blood*. 2013;121(17): 3307-3318.

17. Riesner K, Shi Y, Jacobi A, et al. Initiation of acute graft-versus-host disease by angiogenesis. *Blood*. 2017;129(14):2021-2032.

18. Spoerl S, Mathew NR, Bscheider M, et al. Activity of therapeutic JAK 1/2 blockade in graft-versus-host disease. *Blood*. 2014; 123(24):3832-3842.

19. Shimoda K, Feng J, Murakami H, et al. Jak1 plays an essential role for receptor phosphorylation and Stat activation in response to granulocyte colony-stimulating factor. *Blood*. 1997;90(2):597-604.

20. Pham AH, McCaffery JM, Chan DC. Mouse lines with photo-activatable mitochondria to study mitochondrial dynamics. *Genesis*. 2012;50(11):833-843.

21. Hülsdünker J, Zeiser R. In Vivo Myeloperoxidase Imaging and Flow Cytometry Analysis of Intestinal Myeloid Cells. *Methods Mol Biol*. 2016;1422:161-167.

22. Giroux M, Delisle JS, Gauthier SD, et al. SMAD3 prevents graft-versus-host disease by restraining Th1 differentiation and granulocyte-mediated tissue damage. *Blood*. 2011;117(5):1734-1744.

23. Schiwon M, Weisheit C, Franken L, et al. Crosstalk between sentinel and helper macrophages permits neutrophil migration into infected uroepithelium. *Cell*. 2014;156(3):456-468.

24. Talbot J, Bianchini FJ, Nascimento DC, et al. CCR2 Expression in Neutrophils Plays a Critical Role in Their Migration Into the Joints in Rheumatoid Arthritis. *Arthritis Rheumatol*. 2015;67(7):1751-1759.

25. Lämmermann T, Afonso PV, Angermann BR, Wang JM, Kastenmüller W, Parent CA, Germain RN. Neutrophil swarms require LTB4 and integrins at sites of cell death in vivo. *Nature*. 2013;498(7454):371-375.

26. Mathewson ND, Jenq R, Mathew AV, et al. Gut microbiome-derived metabolites modulate intestinal epithelial cell damage and mitigate graft-versus-host disease. *Nat Immunol*. 2016;17(5):505-513.

27. Koyama M, Cheong M, Markey KA, et al. Donor colonic CD103+ dendritic cells determine the severity of acute graft-versus-host disease. *J Exp Med*. 2015;212(8):1303-1321.

28. Beauvillain C, Delneste Y, Scotet M, et al. Neutrophils efficiently cross-prime naive T cells in vivo. *Blood*. 2007;110(8):2965-2973.

29. Koyama M, Kuns RD, Olver SD, et al. Recipient nonhematopoietic antigen-presenting cells are sufficient to induce lethal acute graft-versus-host disease. *Nat Med*. 2011; 18(1):135-142.

30. Wilhelm K, Ganesan J, Müller T, et al. Graft-versus-host disease is enhanced by extracellular ATP activating P2X7R. *Nat Med*. 2010; 16(12):1434-1438.

31. Jankovic D, Ganesan J, Bscheider M, et al. The Nlrp3 inflammasome regulates acute graft-versus-host disease. *J Exp Med*. 2013;210(10): 1899-1910.

32. Zhong X, Zhu F, Qiao J, et al. The impact of P2X7 receptor antagonist, brilliant blue G on graft-versus-host disease in mice after allogeneic hematopoietic stem cell transplantation. *Cell Immunol*. 2016;310: 71-77.

33. Ostanin DV, Kurmaeva E, Furr K, et al. Acquisition of antigen-presenting functions by neutrophils isolated from mice with chronic colitis. *J Immunol*. 2012;188(3):1491-1502.

34. Wallace JL, McKnight, W., Asfaha, S., Liu, D. Y. Reduction of acute and reactivated colitis in rats by an inhibitor of neutrophil activation. *Am J Physiol*. 1998;274(5 Pt 1): G802-G808.

35. Hampton HR, Bailey J, Tomura M, Brink R, Chtanova T. Microbe-dependent lymphatic migration of neutrophils modulates lymphocyte proliferation in lymph nodes. *Nat Commun*. 2015;6(1):7139.

36. Stickel N, Hanke K, Marschner D, et al. MicroRNA-146a reduces MHC-II expression via targeting JAK/STAT signaling in dendritic cells after stem cell transplantation. *Leukemia*. 2017;31(12):2732-2741.

2018 131: 1858-1869
doi:10.1182/blood-2017-10-812891 originally published online February 20, 2018

Neutrophils provide cellular communication between ileum and mesenteric lymph nodes at graft-versus-host disease onset

Jan Hülsdünker, Katja J. Ottmüller, Hannes P. Neeff, Motoko Koyama, Zhan Gao, Oliver S. Thomas, Marie Follo, Ali Al-Ahmad, Gabriele Prinz, Sandra Duquesne, Heide Dierbach, Susanne Kirschnek, Tim Lämmermann, Martin J. Blaser, Brian T. Fife, Bruce R. Blazar, Andreas Beilhack, Geoffrey R. Hill, Georg Häcker and Robert Zeiser

Blood (print ISSN 0006-4971, online ISSN 1528-0020), is published weekly by the American Society of Hematology, 2021 L St, NW, Suite 900, Washington DC 20036.